◆ Human Brain Mapping 35:2435–2447 (2014) ◆

Reappraisal of the Anatomical Landmarks of Motor and Premotor Cortical Regions for Image-Guided Brain Navigation in TMS Practice

Rechdi Ahdab,[1,2,3] Samar S. Ayache,[1,2] Wassim H. Farhat,[1,2] Veit Mylius,[1,4] Sein Schmidt,[5] Pierre Brugières,[6] and Jean-Pascal Lefaucheur[1,2]*

[1]*EA 4391, Excitabilité Nerveuse et Thérapeutique, Université Paris-Est-Créteil, Créteil, France*
[2]*Service de Physiologie–Explorations Fonctionnelles, Hôpital Henri Mondor, Assistance Publique–Hôpitaux de Paris, Créteil, France*
[3]*Neuroscience Department, University Medical Center Rizk Hospital, Beirut, Lebanon*
[4]*Department of Neurology, Philipps University Marburg, Germany*
[5]*Department of Neurology, Charité Campus, Berlin, Germany*
[6]*Service de Neuroradiologie, Hôpital Henri Mondor, Assistance Publique–Hôpitaux de Paris, Créteil, France*

Abstract: Image-guided navigation systems dedicated to transcranial magnetic stimulation (TMS) have been recently developed and offer the possibility to visualize directly the anatomical structure to be stimulated. Performing navigated TMS requires a perfect knowledge of cortical anatomy, which is very variable between subjects. This study aimed at providing a detailed description of sulcal and gyral anatomy of motor cortical regions with special interest to the inter-individual variability of sulci. We attempted to identify the most stable structures, which can serve as anatomical landmarks for motor cortex mapping in navigated TMS practice. We analyzed the 3D reconstruction of 50 consecutive healthy adult brains (100 hemispheres). Different variants were identified regarding sulcal morphology, but several anatomical structures were found to be remarkably stable (four on dorsoventral axis and five on rostrocaudal axis). These landmarks were used to define a grid of 12 squares, which covered motor cortical regions. This grid was used to perform motor cortical mapping with navigated TMS in 12 healthy subjects from our cohort. The stereotactic coordinates (*x-y-z*) of the center of each of the 12 squares of the mapping grid were expressed into the standard Talairach space to determine the corresponding functional areas. We found that the regions whose stimulation produced almost constantly motor evoked potentials mainly correspond to the primary motor cortex, with rostral extension to premotor cortex and caudal extension to posterior parietal cortex. Our anatomy-based approach should facilitate the expression and the comparison of the results obtained in motor mapping studies using navigated TMS. *Hum Brain Mapp 35:2435–2447, 2014.* **© 2013 Wiley Periodicals, Inc.**

Key words: motor cortex; premotor cortex; sulcal anatomy; transcranial magnetic stimulation

*Correspondence to: J.P. Lefaucheur, Service de Physiologie–Explorations Fonctionnelles, Hôpital Henri Mondor, 51 avenue de Lattre de Tassigny, 94010 Créteil, France.
E-mail: jean-pascal.lefaucheur@hmn.aphp.fr

Received for publication 18 February 2013; Revised 14 April 2013; Accepted 20 May 2013.
DOI: 10.1002/hbm.22339
Published online 3 September 2013 in Wiley Online Library (wileyonlinelibrary.com).

© 2013 Wiley Periodicals, Inc.

INTRODUCTION

Transcranial magnetic stimulation (TMS) is a neurophysiological technique that offers the possibility to study various neural functions and to map their cortical representation. The accuracy of TMS mapping is thought to be improved by the use of recently developed navigation systems that integrate cerebral imaging data, magnetic resonance imaging (MRI), or positron emission tomography [Lefaucheur, 2010]. However, to perform navigated TMS requires a perfect knowledge of the anatomical landmarks of the cortical surface and the location of some of these landmarks may be highly variable from one brain to another. In this work, we studied the anatomy of the motor and premotor cortical regions in a series of normal brain MRIs and we sought to identify the most stable structures, which could serve as anatomical landmarks for mapping motor cortical regions in navigated TMS practice.

SUBJECTS AND METHODS

Anatomical Study of Motor Cortical Regions on Normal Brain MRIs

For this study, we analyzed 50 healthy adult brains (100 hemispheres) from 15 women and 35 men, aged from 23 to 88 years (mean 45 years). These brains were extracted from our navigated TMS database and the study was approved by the local IRB. Three-dimensional (3D) brain reconstructions were generated with a TMS-dedicated navigation system (eXimia NBS, Nexstim Oy, Helsinki, Finland) by loading 160 1 mm-thick T1-weighted native MRI slices acquired with the following parameters: TR = 2250.00 ms, TE = 2.60 ms, TI: 900 ms, FOV: 240.000, Flip Angle = 9°, 240 × 256 matrix, voxel size 1.0 × 1.0 × 1.0 mm.

Analysis of the morphology of the sulci and identification of the anatomical variants were performed on 3D brain reconstructions viewed at a peeling depth ranging from 2 to 3 cm. Working at this depth offers various advantages. First, some important sulci are merged at the surface and can be individualized only at a certain depth [Chiavaras and Petrides, 2000; Ono et al., 1990] (Fig. 1A,B). Conversely, some superficial secondary sulci, which are too variable to be retained as anatomical landmarks, are superficial and disappear in depth (Fig. 1C,D). Instead of proposing a detailed anatomical description of the cortical surface, we sought to identify the most stable structures that might serve as anatomical landmarks in motor mapping using navigated TMS. Consequently, our description of the gyri and sulci may seem quite different from what anatomists usually report.

Motor Evoked Potentials and Stereotactic Normalization

From the anatomical study, we determined the existence of stable landmarks in the motor cortical region, from which a grid was drawn. This grid was used to perform TMS mapping in a standardized way. To illustrate the value of this approach, motor cortical mapping was performed in 12 healthy subjects from our cohort, 5 women and 7 men, aged 24–45 years (mean 28 years). TMS was delivered using a figure-8 coil type B65 connected to a MagOption ×100 stimulator [MagVenture (Mag2Health), Farum, Denmark]. The stimulation coil was positioned tangentially to the scalp and oriented perpendicular to the central sulcus (CS). Electromyographic recordings were made using self-adhesive surface electrodes placed over the first dorsal interosseus muscle of the right hand (left hemisphere stimulation). Motor evoked potentials (MEPs) were filtered, amplified and stored for analysis using a device (ME6000, Mega Electronics Inc., Kuopio, Finland) dedicated to MEP recording and coupled with the navigation system. The stimulation intensity was set at 120% of rest motor threshold, which was determined according to usual method [Rossini et al., 1994].

The TMS mapping grid we created consisted of 12 squares. The 3D-space anatomical coordinates (*x*-*y*-*z*) of the center of each of these 12 squares were recorded. The Eximia NBS system provides anatomical coordinates in the so-called "MRI coordinate" system, based on a bounding box for the brain of 200 × 250 × 250 mm with an origin (0, 0, 0) located at the right inferior-posterior edge of the box. The x-axis is oriented from the right (0) to the left ear. The y-axis is oriented from the neck (0) to the top of the head. The z-axis is oriented from inion (0) to nasion. Then, brain coordinates were transformed from the "MRI coordinate system" into the space defined by the ICBM NIH, P-20 project space that approximates the space defined by the Talairach and Tournoux atlas [Talairach and Tournoux, 1988]. A 12-parameter affine transformation of the individual coordinates was estimated through the spatial normalization of each MRI sequence within a Bayesian framework using discrete cosine transform basis functions as implemented in the software package SPM8 [Ashburner and Friston, 1999]. In the Talairach space system, the x coordinates are defined on the right/left (+/−) axis, the y coordinates on the rostral/caudal (+/−) axis, and the z coordinates on the dorsal/ventral (+/−) axis, with the anterior commissure serving as the reference point ($x = y = z = 0$) [Talairach and Tournoux, 1988]. According to the Talairach and Tournoux atlas, we determined the anatomical correspondence of each square of our mapping grid in terms of Brodmann area (BA).

RESULTS

Central Sulcus

The CS represents the anatomical limit between the frontal lobe and the parietal lobe. Its anterior margin is occupied by the primary motor cortex (M1). This structure, remarkably stable, was identified in 100% of the brains we studied. Its depth ranged from 34 to 44 mm (mean ± SD: 37.8 ± 2.7). Within the CS, the representation of the hand, called the "hand knob," presents a very specific morphology, like an inverted

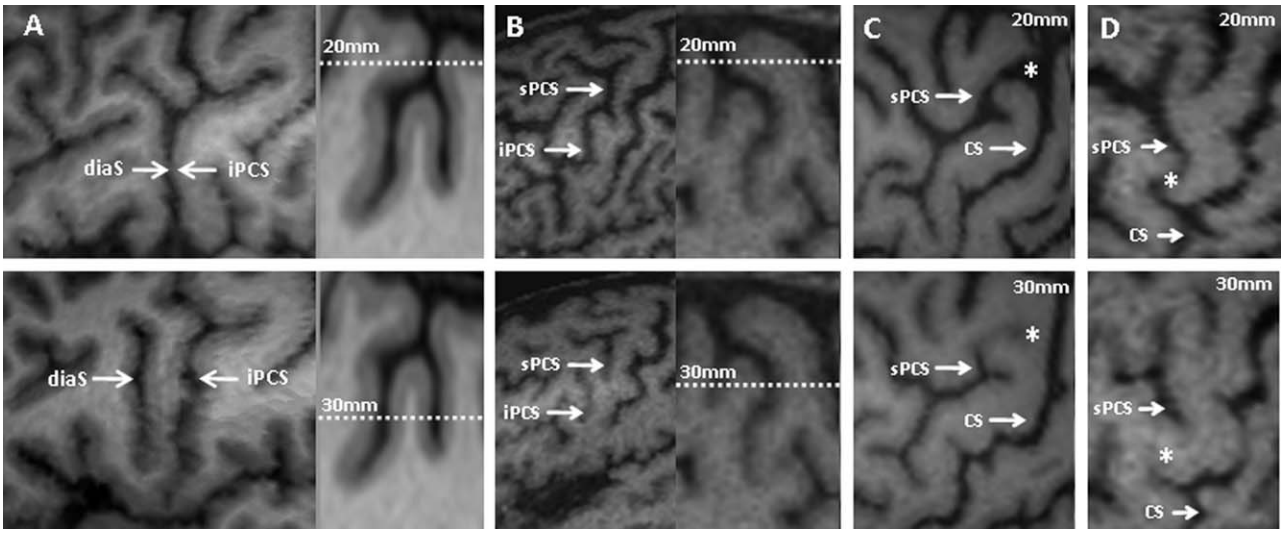

Figure 1.

(**A**,**B**) Examples of clearly separated sulci at a certain depth of the brain that merge at the surface of the cortex. (**C**,**D**) Examples of sulci observed at the cortical surface and not observed deeper. diaS: diagonal sulcus; iPCS: inferior precentral sulcus; sPCS: superior precentral sulcus; CS: central sulcus; *: a superficial sulcus linking the sPCS to the CS.

"omega" [Yousry et al., 1997] (Fig. 2). In some cases (13% in our series), the "omega" was replaced by an "epsilon" (Fig. 2E). The CS comprises three segments: a superior (dorsal) genu, a middle genu, and an inferior (ventral) genu [Yousry et al., 1997]. An interdigitation of the walls of the precentral and postcentral gyri is at the origin of this aspect. The hand knob is located in the middle genu of the CS, which is the seat of an outgrowth of the precentral gyrus that may produce an apparent discontinuity of the CS [White et al., 1997] (Fig. 2A,D). In our series, the "omega" shape of the CS at the hand knob and the apparent discontinuity of the CS at its bottom was observed in 81% of cases (Fig. 2A). Only one of these two features was present in 16% of the subjects (Fig. 2B,D). Finally, we failed to identify these characteristics of the middle genu of the CS in only 3% of cases (Fig. 2C). The inferior part of the "omega" and the apparent discontinuity of the CS were usually located at a level on the dorsoventral axis where there is also the intersection between the superior frontal sulcus (sFS) and the precentral sulcus (PCS).

The inferior part of the CS has a much more variable morphology. It presents two to four curvatures and generally breaks before reaching the sylvian fissure (SF) [Fesl et al., 2003]. This segment corresponds to the motor representation of the face and tongue, but unlike the hand, there is no particular CS morphology to identify these motor regions [Fesl et al., 2003].

Precentral Sulcus

The anterior border of the precentral gyrus is defined by a series of sulci, globally called the PCS, which is a deep sulcus (30 to 40 mm, like the CS), constantly present and easy to identify in 100% of the cases. The PCS usually comprises two separate sulci, the superior and inferior PCS (sPCS and iPCS), corresponding to a posterior bifurcation of the sFS and the inferior frontal sulcus (iFS), respectively [Turner, 1948]. Therefore, the PCS of the adult brain is typically broken at a dorsoventral level corresponding to the middle frontal gyrus (F2; 77% of the cases in our series), leading to a continuity between F2 and the precentral gyrus (Fig. 3). The major part of the sPCS is caudal to the iPCS. Less commonly, the PCS seems unbroken, corresponding to a single sulcus (23%), at least at the surface of the cortex. However, we constantly found the presence of two separated sulci, sPCS, and iPCS, at a greater depth (Fig. 1B).

The sPCS separates the precentral gyrus from the superior frontal gyrus (F1) and the superior part of F2. The sPCS is usually made of two distinct segments: one dorsal (more caudal) and the other ventral (more rostral). These two segments merge most frequently with the sFS, appearing as a single sulcus (Fig. 4A). The sPCS rarely reaches the interhemispheric fissure (IHF; 19%; Fig. 4B). At this level, the sPCS usually leaves room for the median PCS (mePCS), which was identified in 97% of the cases and extends to the median aspect of the hemisphere [Germann et al., 2005]. Finally, the sPCS can have a more complex structure with several branches (Fig. 4E) or it can more rarely appear detached from the sFS (Fig. 4F).

In this region, two other sulci can also be identified, which are more superficial and run less deeply into the brain than the CS and the PCS. First, there is the paramedian sulcus (paraS), which is a horizontal sulcus located in F1 between the IHF and the sFS, parallel to them and

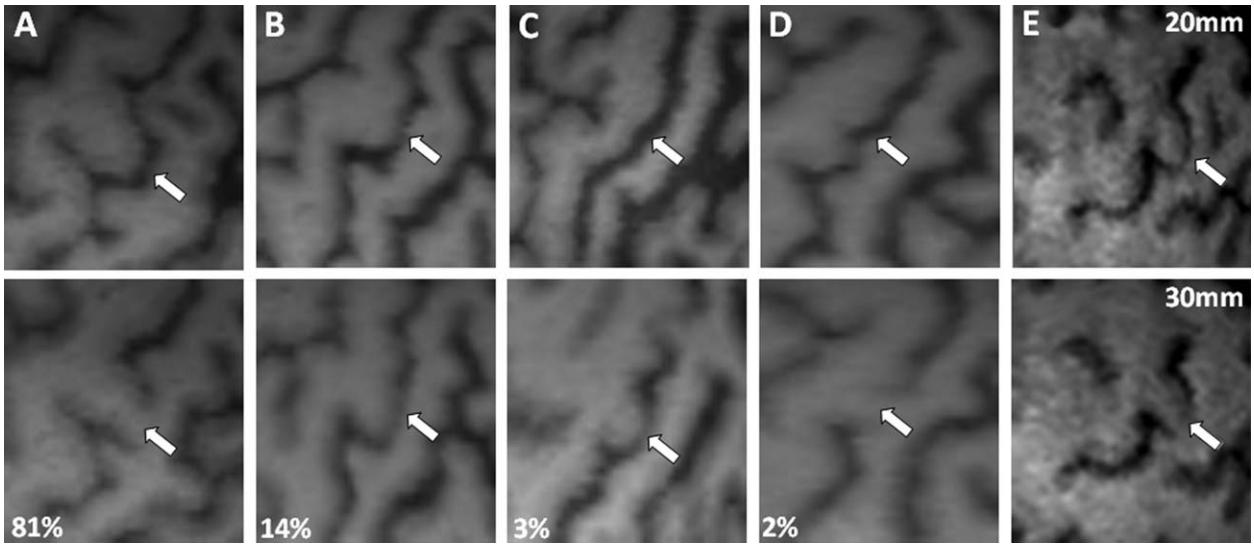

Figure 2.
Morphology of the CS at the level of hand representation, usually characterized by an inverted "omega" aspect (**A**,**B**). In some cases, an interruption of the CS can be observed at a depth of 30 mm (**A,D**). In other cases, the "omega" aspect is absent (**C**,**D**) or replaced by an "epsilon" aspect (**E**).

present in 91% of the cases (Fig. 3). Second, there is the marginal PCS (maPCS), which is a vertical sulcus located in the precentral gyrus between the sPCS and the CS, parallel to them and present in 61% of the cases (Fig. 3).

The iPCS separates the precentral gyrus from the inferior part of F2 and the inferior frontal gyrus (F3). It comprises three segments: one dorsal and one ventral, more or less vertical, and one horizontal. These three segments were merged into a single structure in 75% of the cases. The dorsal segment of the iPCS is fairly long and meanders over a variable distance in F2, most frequently rostral to the ventral segment of the sPCS but caudal to the ventral segment of the iPCS. The horizontal segment of the iPCS (hiPCS) extends over a variable distance rostrally in F2 and therefore may be mistaken for the iFS. We were able to clearly distinguish between these two sulci in 72% of the cases, the hiPCS being more dorsal and caudal than the iFS (Fig. 5A,B). In the other cases, these sulci appeared to be continuous (Fig. 5C).

The correct identification of the dorsal and horizontal branches of the iPCS may be difficult due to the presence of a middle frontal sulcus, between the sFS and the iFS, in the posterior part of F2. In contrast, the ventral branch of the iPCS has a perfectly constant linear morphology. Its course is roughly parallel to the CS and ends at a variable distance of the SF. In some cases, it merges inferiorly with the diagonal sulcus (diaS; Fig. 1A).

Inferior (IFS) and Superior (SFS) Frontal Sulci

Only the caudal parts of the frontal sulci were analyzed in this study, since these sulci extend rostrally far beyond the motor areas. The sFS has a course parallel to the IHF. Caudally, it merges into the sPCS forming a T-shaped branching in 77% of the cases (Fig. 4D). Less commonly, it crosses the sPCS and briefly continues posterior to it (15%; Fig. 4E), or it breaks prematurely without reaching the sPCS (8%; Fig. 4F). Although this sulcus is generally continuous, it can be broken in its middle or caudal segment (33%).

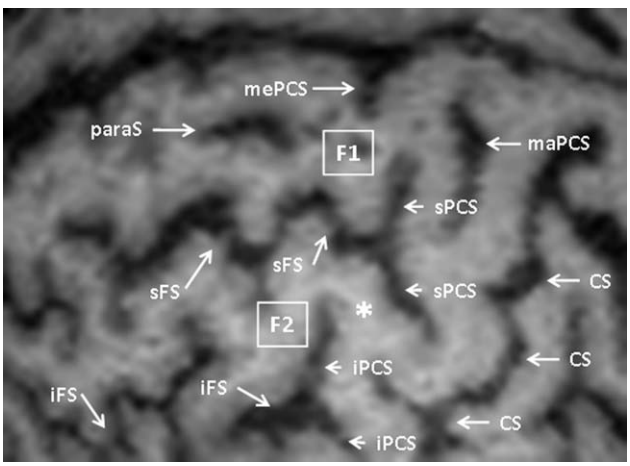

Figure 3.
Break of the PCS between its superior (sPCS) and inferior (iPCS) segments (*). paraS: paramedian sulcus; mePCS: median precentral sulcus; maPCS: marginal precentral sulcus; F1: superior frontal gyrus; F2: middle frontal gyrus; sFS: superior frontal sulcus; iFS: inferior frontal sulcus; CS: central sulcus.

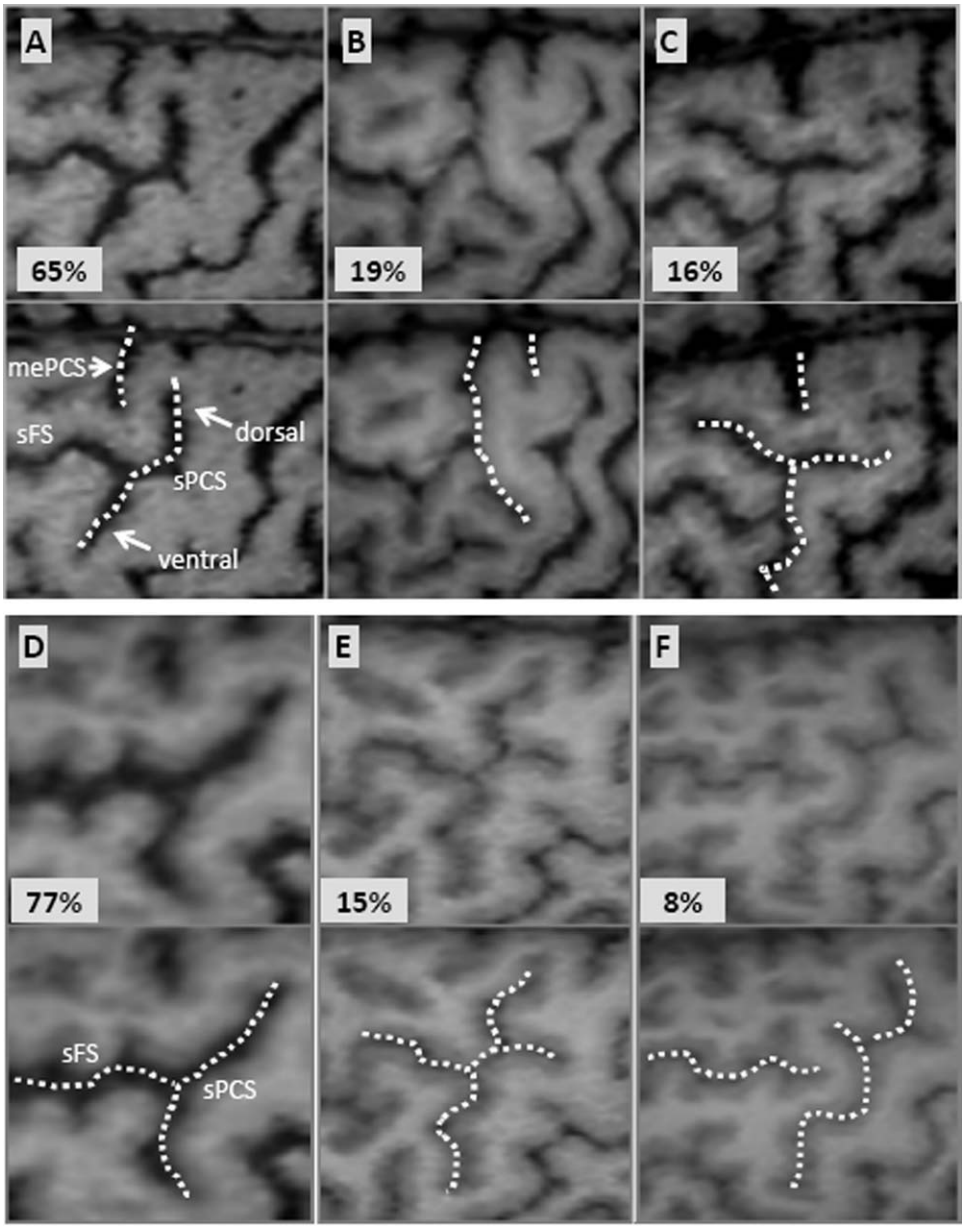

Figure 4.
The morphological variants of the superior precentral sulcus (sPCS), especially regarding its dorsal and ventral branches (**A**–**C**) and its relationship with the superior frontal sulcus (sFS) (**D**–**F**). mePCS: median precentral sulcus.

The iFS has a course almost parallel to the SF. Caudally, it merges into the iPCS (Fig. 5B,C) or breaks prematurely without reaching it (Fig. 5A). There is sometimes one or two brief breaks in the iFS (22%), complicating its identification.

Ventral to the iFS and rostral to the iPCS, the posterior part of F3 presents a particular segmentation, defined by the ascending and horizontal branches of the SF (aSF and hSF), which subdivide this cortical region into three parts: pars orbitalis (POr), pars triangularis (PTr), and pars opercularis (POp) of F3 (from anterior to posterior; Fig. 6). The POp (between the aSF and the iPCS) is sometimes divided into two parts by a vertical sulcus, the diaS. The PTr (between the hSF and the aSF) may also be divided by a vertical sulcus, the triangular sulcus. The POr is located rostrally to the hSF and is limited anteriorly by the orbital

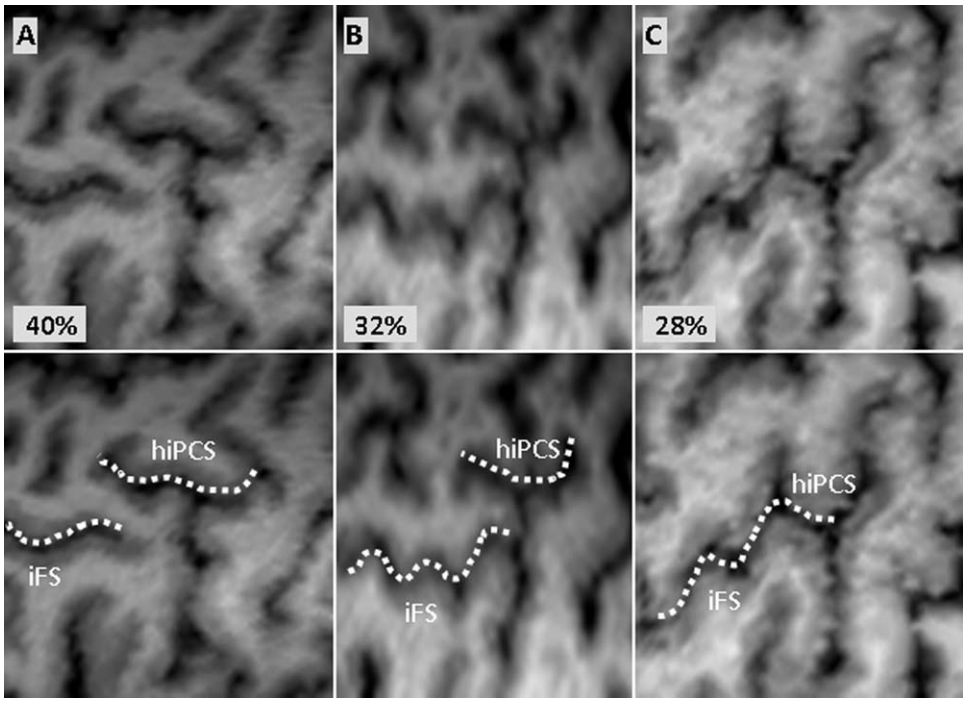

Figure 5.
Relationship between the posterior segment of the inferior frontal sulcus (iFS) and the horizontal branch of the inferior precentral sulcus (hiPCS).

sulcus. The functional importance of this region lies in the fact that it corresponds to the language center (Broca's area) in the dominant hemisphere.

Stable Anatomical Landmarks

Thus, the gyri and sulci in the motor cortical region are far from being constant between individuals. We were even able to observe a certain degree of interhemispheric asymmetry in these structures in more than 90% of the subjects. However, we found that some sulcus segments showed a remarkable stable morphology. For example, the CS with its "omega" shape was remarkably constant at the level of the hand knob, unlike other segments of the CS. The ventral segments of the sPCS and iPCS also showed a very stable morphology: they were almost linear, with a course parallel to the CS and no ramifications (at least at the depth at which this work was done). Thus, we were able to define four stable and easily identifiable cortical landmarks on the dorsoventral axis and five on the rostrocaudal axis (Fig. 7).

On the dorsoventral axis, the most dorsal of the four stable landmarks was the paraS, which is a horizontal sulcus located halfway between the IHF and the sFS. This sulcus was identified in 91% of the cases. The second landmark was the intersection between the sPCS and the sFS (or its caudal prolongation). This region was identified in 100% of the cases. The third landmark was the bottom of the median genu of the hand knob ("omega") of the CS or the apparent break of this latter (identifiable in 97% of the cases). Finally, the most ventral stable landmarks was the intersection between the iPCS and the iFS (or its caudal prolongation), present in 100% of the cases.

Similarly, five stable landmarks were defined on the rostrocaudal axis. These landmarks were from front to back: (i) the aSF; (ii) the intersection between the iPCS and the iFS (or its caudal prolongation); (iii) the intersection between the sPCS and the sFS (or its caudal prolongation); (iv) the bottom of the hand knob ("omega") of the CS (or its apparent break); and (v) the postcentral sulcus (poCS) at a dorsoventral level corresponding to the bottom of the motor hand knob.

Probabilistic Map of the Motor Cortical Region

Using the anatomical landmarks as described above, we were able to draw a grid covering the motor cortical region in each individual (Fig. 7). The purpose of this grid was to help perform TMS mapping in a more standardized manner. We then studied the ability to produce MEPs by delivering navigated TMS pulses at 120% of rest motor threshold in each square of the cortical grid. The percentage of patients in whom MEPs could be obtained in a contralateral hand muscle at the stimulation of a given square was calculated (Fig. 8). Depending on the square, MEPs were obtained in 16–100% of subjects. Finally, we collected the stereotactic coordinates (x, y, and z) of the

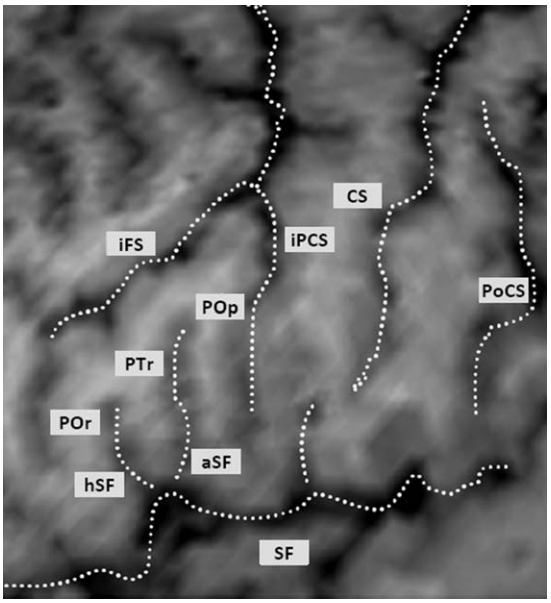

Figure 6.

Organization of the posterior part of the inferior frontal gyrus, including the pars orbitalis (Por), pars triangularis (PTr), and pars opercularis (Pop) separated by the horizontal (hSF) and ascending (aSF) branches of the SF. iFS: inferior frontal sulcus; iPCS: inferior precentral sulcus; CS: central sulcus; PoCS: postcentral sulcus.

center of each square of the grid in the "MRI coordinate" system provided by the navigation system. Then we transferred these coordinates into the "Talairach atlas" system to determine their anatomical correspondence in terms of BA. The mean *x*-*y*-*z* values of the center of each square of the grid in both coordinate systems and the corresponding BAs are presented in Table I. These results were rather symmetrical. The squares providing the highest percentages of hand MEPs were centered on M1/BA 4 (S6–S7), the premotor cortex (PMC)/BA 6 (S10), or the posterior parietal cortex/BA 7 (S11). Although centered on M1, the excitable motor cortical region included large areas of the PMC and portions of the postcentral gyrus.

DISCUSSION

This study highlights the variability of sulcus anatomy in the motor cortical region, except for a few very stable landmarks. The identification of these landmarks (four on the dorsoventral axis and five on the rostrocaudal axis) in individual brains offers the possibility to draw an individualized anatomical grid dividing the cortical surface into squares corresponding to well-defined regions. This segmentation is of great help to overcome the inter-individual variability of brain sulci and to standardize motor cortical mapping with navigated TMS. Indeed, the ability to produce MEPs in response to the stimulation of each of these

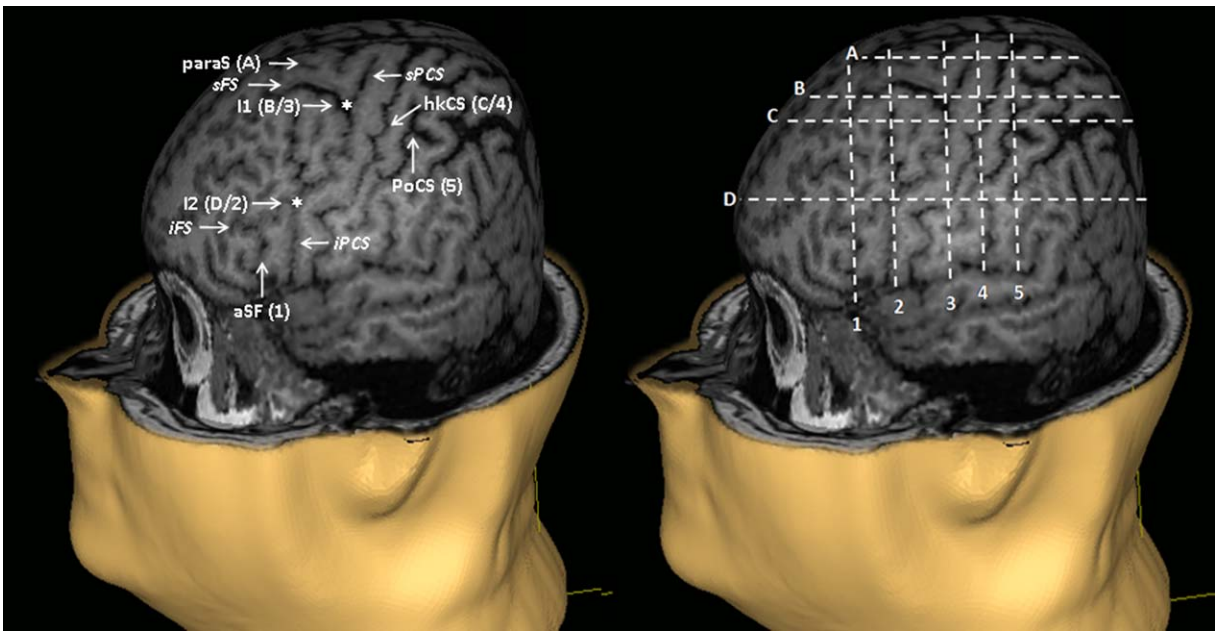

Figure 7.

Segmentation of the motor cortex based on stable anatomical landmarks observed at the cortical surface. paraS: paramedian sulcus; I1: intersection between the superior frontal sulcus (sFS) and the superior precentral sulcus (sPCS); hkCS: hand knob of the CS; I2: intersection between the inferior frontal sulcus (iFS) and the inferior precentral sulcus (iPCS); aSF: ascending branch of the sylvian fissure; PoCS: postcentral sulcus. [Color figure can be viewed in the online issue, which is available at wileyonlinelibrary.com.]

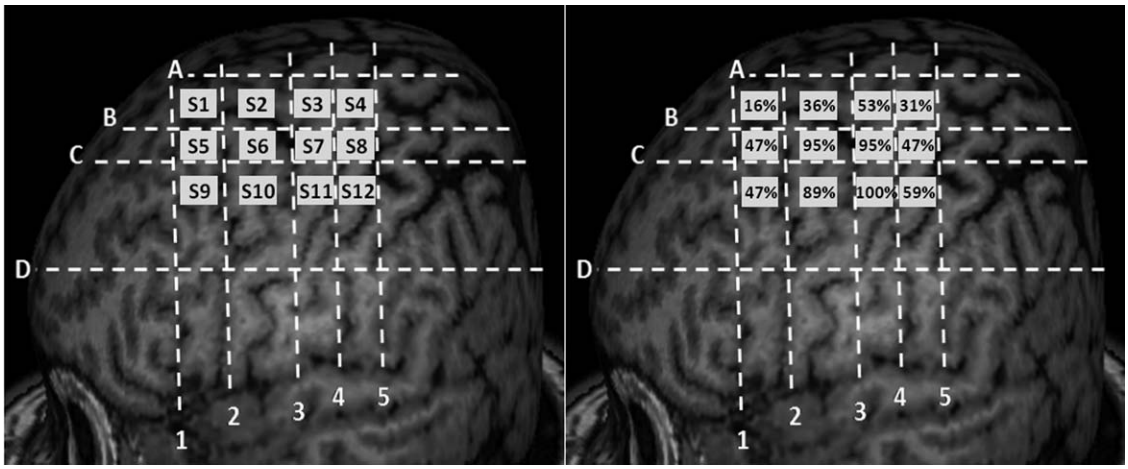

Figure 8.

Segmentation of the motor cortex in 12 squares, based on stable anatomical landmarks. (**A**) Numbered squares of the grid (from S1 to S12). (**B**) Percentages of motor evoked potentials obtained in contralateral hand muscle for the stimulation of each square of the grid in a series of 12 healthy subjects.

regions can be determined at individual level, and then, for a group of subjects, the probability of producing MEPs to the stimulation of a given region can be calculated. This procedure can help study parallel groups or follow a cohort longitudinally by comparing the probability of producing MEPs to the stimulation of each square of the cortical grid. An increased probability of obtaining MEPs to the stimulation of a given square would imply a greater involvement of this cortical region in motor commands, whereas a reduced probability would imply less motor involvement of this region. This can be an interesting approach to demonstrate changes in cortical motor representations and to study cortical plasticity. However, other factors change the susceptibility of the cortex to be activated by the TMS pulse and should be taken into account, such as the interaction between the spatial diffusion of the electrical field generated into the brain and the intrinsic excitability of the cerebral tissue. Another important point is the influence of various technical parameters of TMS, such as stimulation intensity, coil type, and coil orientation, on the motor maps provided by this technique, as illustrated in Figure 9.

We applied the mapping procedure as described above in a series of healthy subjects using the proposed grid. We found that the generation of MEPs was not restricted to the stimulation of M1. This is related to several factors including those inherent to the technique of TMS, such as the diffusion of the induced currents into the brain and the propensity of TMS to activate axons of neural circuits rather than local cell bodies [Lefaucheur, 2008, 2012]. A recent study comparing motor cortical mapping using navigated TMS and movement-related fMRI signal changes showed that the information provided by TMS does not only reflect motor function at the stimulation site but also interactions with remote areas in the entire motor system [Sarfeld et al., 2012]. In a previous study, we found that the site of cortical stimulation producing MEPs of maximal amplitude in contralateral hand muscles (hand motor hotspot) was located in the precentral gyrus, often more anterior than hand knob location [Ahdab et al., 2010]. In this study, the cortical regions whose stimulation was most constantly associated with MEPs corresponded to M1, including the hand knob. However, MEPs could be obtained to the stimulation of a large cortical region, with a caudal extension to PPC and a rostral extension to PMC, according to Talairach and Tournoux atlas [Talairach and Tournoux, 1988]. In this regard, the border between M1 and PMC is a particularly debated matter in the literature. Therefore, defining the anatomical limits of PMC deserves an updated review.

Anatomical Limits of the PMC

The PMC is divided into six functional areas, four of which occupy the lateral surface of the frontal lobe: the dorsal (dPMC) and ventral (vPMC) PMC, the supplementary motor area (SMA), and the area anterior to the SMA (pre-SMA) [Rizzolatti and Luppino, 2001].

Anatomically, the rostral limit of the PMC is anterior to the PCS in humans, variable from one individual to another, and does not actually correspond to any identifiable anatomical landmark [Geyer, 2004]. The rostral extension of the PMC is even larger on the medial side of the hemispheres [Amunts et al., 1999].

The definition of the caudal limit of the PMC, which is the rostral limit of M1, is also controversial, even at the cytoarchitectonic level [Roland and Zilles, 1996]. The presence of large pyramidal cells (Betz cells, in layer V) characterizes M1. However, from M1 to PMC, there is a

TABLE I. Mean stereotactic coordinates of the center of each square of the grid used to map the motor cortical regions, expressed in MRI and Talairach space coordinate systems, with the corresponding BA

	MRI coordinates (mm)			Talairach coordinates (mm)			BA
Right	*x*	*y*	*z*	*x*	*y*	*z*	
S1	63.3	216.3	128.0	15.6	8.5	60.4	Anterior border of BA 4
S2	59.4	217.7	113.7	20.5	−5.7	63.3	BA 4
S3	56.1	218.2	97.3	24.8	−22.2	65.0	Posterior border of BA 4
S4	55.9	218.0	84.8	25.7	−34.9	65.5	BA 5
S5	53.6	211.3	128.7	26.4	9.6	54.5	Posterior border of BA 6
S6	50.0	212.3	115.6	30.9	−3.5	56.7	Anterior border of BA 4
S7	47.1	212.8	99.1	34.8	−20.0	58.5	BA 4
S8	46.2	212.4	86.1	36.5	−33.2	58.8	Border between BA 5 and BA 7
S9	41.9	201.4	130.8	39.4	11.9	42.5	BA 6
S10	38.3	202.1	116.9	43.9	−1.9	44.4	Posterior border of BA 6
S11	35.9	202.7	100.1	47.2	−18.9	46.3	Border between BA 2 and BA 7
S12	35.2	201.9	87.8	48.6	−31.4	46.1	BA 7
Left							
S1	92.0	218.2	127.2	−15.7	6.6	62.5	Posterior border of BA 6
S2	96.8	219.0	115.2	−20.6	−5.7	64.2	BA 4
S3	102.9	218.9	98.8	−26.5	−22.6	65.1	Posterior border of BA 4
S4	104.9	218.3	84.2	−28.0	−37.6	65.2	BA 5
S5	100.6	213.3	128.7	−25.2	7.6	56.3	Posterior border of BA 6
S6	105.7	213.3	116.7	−30.2	−4.7	57.1	BA 4
S7	110.8	213.3	100.9	−35.1	−20.9	58.1	Posterior border of BA 4
S8	112.6	213.3	86.5	−36.4	−35.7	58.8	Border between BA 5 and BA 7
S9	113.8	200.6	131.8	−39.3	9.9	40.5	BA 6
S10	124.0	201.3	119.8	−50.1	−2.6	41.9	Posterior border of BA 6
S11	123.1	201.6	103.6	−48.4	−19.0	43.6	Anterior border of BA 7
S12	126.1	200.8	89.1	−51.0	−34.0	43.4	BA 7

progressive decrease in the number of Betz cells rather than an abrupt disappearance [Wang et al., 2001; White et al., 1997]. Initially, Brodmann proposed that M1 extended rostrally to the whole convexity of the precentral gyrus (area 4), but recent histological studies showed that M1 occupies the anterior wall of the CS and only a limited part of the exposed surface of the precentral gyrus, namely in its dorsomedial part [Geyer et al., 2000; Rademacher et al., 2001]. Ventrally, M1 is buried in the depth of the CS [White et al., 1997].

On the dorsal border of the PMC, the SMA and the dPMC have been recognized as two distinct functional regions [Penfield and Welch, 1951], but difficult to distinguish on anatomical grounds [Matelli et al., 1985]. In fact, the SMA is located on the mesial part of the hemispheres, extending only a little on the lateral surface of the hemisphere [Grafton et al., 1996; Mayka et al., 2006; Tanji and Hoshi, 2009].

Ventrally, the distinction between the dPMC and the vPMC was not mentioned in human nomenclature until very recently. However, based on histological and functional criteria, it is certain that the PMC consists of two distinct areas, one ventral and the other dorsal. The virtual line corresponding to the posterior prolongation of the iFS to the CS was generally used as the limit between those two areas, according to hypothetical homologies between humans and primates. Rizzolatti et al. [1998] suggested that the limit between the dPMC and the vPMC was much more dorsal. Recent work based on brain imaging [Mayka et al., 2006; Schubotz et al., 2010; Tomassini et al., 2007] seem to confirm this hypothesis.

All these data provided by the literature on the anatomical boundaries of PMC, especially regarding the dPMC, are summarized in Figures 10 and 11 and Table II.

Implication of This Work to the Practice of Navigated TMS

As mentioned above, one interesting application of this study should be the use of our cortical grid to determine the probability of obtaining MEPs to the stimulation of well-defined cortical regions. Another relevant application should be the distinction made between M1 and PMC areas. We propose to strictly define the M1 target as the anterior bank of the CS, using the following segmentation along the dorsoventral axis: trunk and lower limb representation being more medial than the level of projection of the sFS (F1 level); hand and upper limb representation being located between the levels of projection of the sFS and the iFS (F2 level); and the representation of the face being more lateral than the level of projection of the iFS (F3 level) [Nguyen et al., 1999].

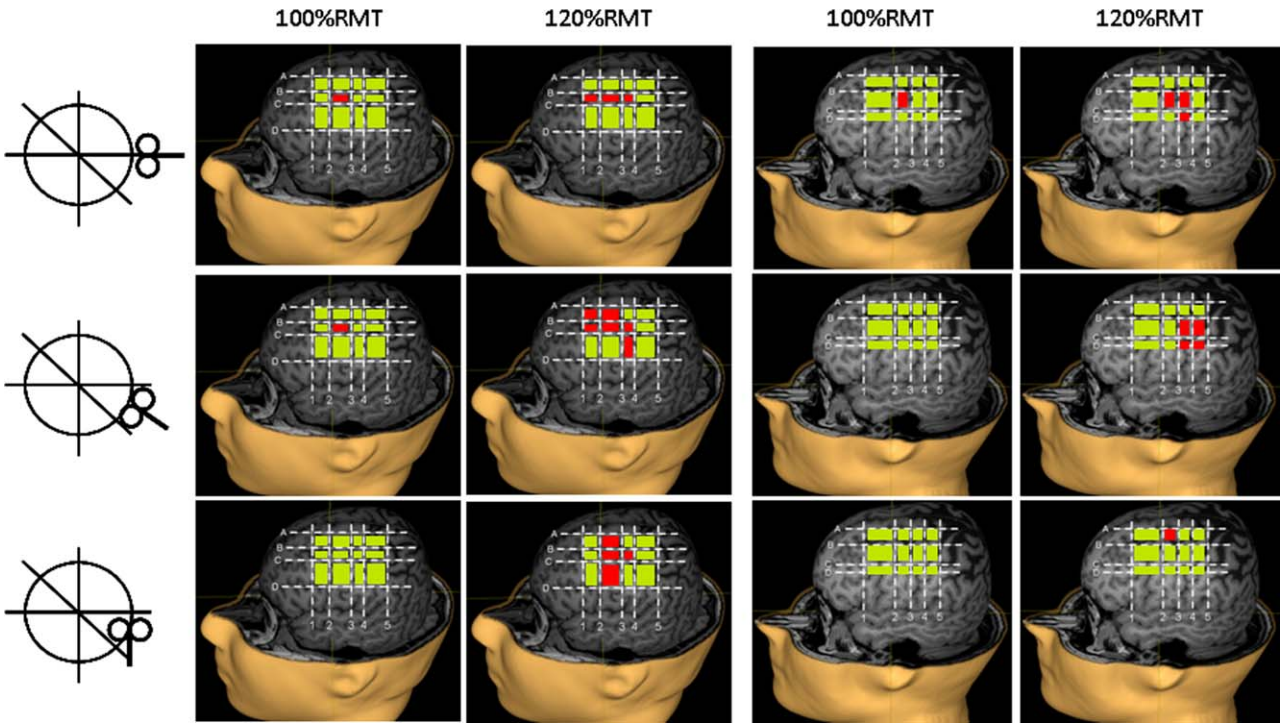

Figure 9.

Influence of coil orientation (postero-anterior, 45°, or latero-medial) and stimulation intensity (100% or 120% of rest motor threshold, RMT) on motor maps on the left hemisphere of two subjects. The squares whose stimulation produced motor evoked potentials are shown in red, and those whose stimulation produced no responses are shown in green. [Color figure can be viewed in the online issue, which is available at wileyonlinelibrary.com.]

Concerning the dPMC, fMRI data showed that its center of activation corresponds to the dorsal segment of the sPCS [Amiez et al., 2006; Grol et al., 2006; Toni et al., 2001]. This is also consistent with some TMS data [Johansen-Berg et al., 2002; Schluter et al., 1998]. Consequently, we propose to choose the dorsal portion of the sPCS (above the sFS) as the landmark for targeting the dPMC (Fig. 11).

Concerning the vPMC, fMRI data showed that its center of activation corresponds to the ventral segment of the iPCS [Binkofski et al., 1999; de Jong et al., 2001, Ehrsson et al., 2003]. Consequently, we propose to choose the ventral portion of the iPCS (below the iFS) as the landmark for targeting the vPMC (Fig. 11).

Concerning the SMA and pre-SMA, the problem is much more complicated. These two structures are mostly situated in the mesial part of the hemispheres and extend only a little onto the lateral surface of the hemispheres. At this level, the SMA would be situated at a rostrocaudal level corresponding to the paracentral branch of the cingulate sulcus [Fink et al., 1997; Grafton et al., 1996] while the pre-SMA would be situated immediately anterior to the ventral anterior commissural line. Since the degree of lateral extension of the SMA is impossible to determine, we propose to consider only a narrow band of the lateral

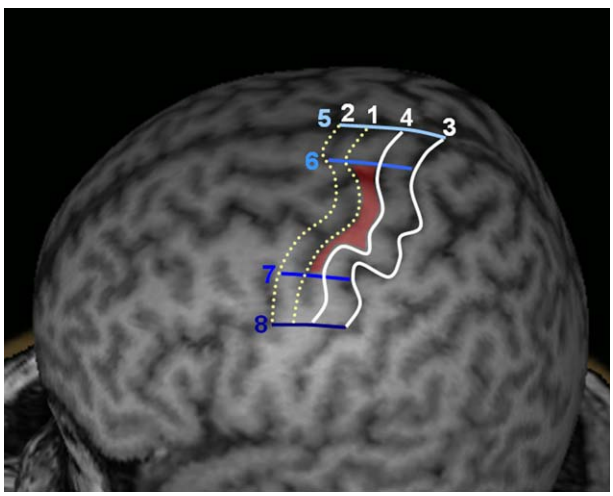

Figure 10.

Definition of the anatomical limits of the dPMC (red shade) according to literature data. Numbers refer to references listed in Table II. [Color figure can be viewed in the online issue, which is available at wileyonlinelibrary.com.]

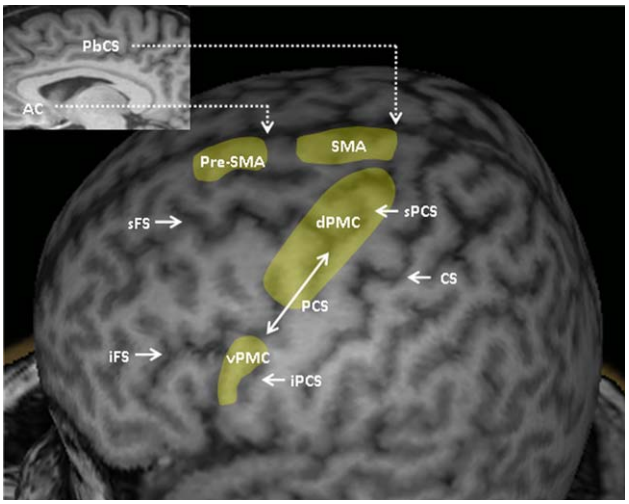

Figure 11.
Representative areas corresponding to the PMC, including its dorsal (dPMC) and ventral (vPMC) parts. AC: anterior commissure; PbCS: paracentral branch of the cingulate sulcus; SMA: supplementary motor area; sFS: superior frontal sulcus; iFS: inferior frontal sulcus; sPCS: superior precentral sulcus; PCS: precentral sulcus; iPCS: inferior precentral sulcus; CS: central sulcus. [Color figure can be viewed in the online issue, which is available at wileyonlinelibrary.com.]

surface of the frontal cortex as belonging to the SMA and the pre-SMA (Fig. 11).

CONCLUSION

Despite high interindividual variability in sulcus anatomy, we were able to define several stable landmarks in the motor cortical region, based on the study of a large series of healthy brains with an image-guided navigation system dedicated to TMS use. The grid, drawn from these landmarks and overlying the motor cortex, offers the possibility to get TMS maps in a very standardized manner. The reproducibility of these maps when performed by different investigators, their repeatability when performed several times for the same subject and their variability (comparability) among subjects are several issues that need to be addressed in further study.

Our targeting method was based on individual morphological brain imaging, while other methods are based on functional neuroimaging [Diekhoff et al., 2011] or probabilistic strategy [Paus et al., 1997]. This latter method takes into account the probabilistic location of a given cortical region in a standard reference space from meta-analysis of functional neuroimaging studies. Then, the resulting x, y, and z coordinates are transformed into coordinates in the "native" space of the subject brain. This method has two disadvantages compared to ours, which are: (i) defining targets in a standardized space, with the associated error due to the distortion induced by standardization, (ii) defining targets from group statistics, without considering inter-individual variability of brain anatomy. Regarding functional neuroimaging, correlations were found between regions of activation and structural brain anatomy, including cytoarchitectonic data [Eickhoff et al., 2005, 2006, 2007]. However, the main limitations of this approach relate to the specificity of the task used to induce brain signal changes and to the way of acquiring and analyzing the imaging data, which can have various pitfalls according to the methods [Diekhoff et al., 2011; Eickhoff et al., 2007; Thyreau et al., 2012].

Our navigated TMS mapping technique is based on a grid, drawn over the cortical surface from stable anatomical landmarks defined on 3D brain reconstruction and can be generalized and extended to cortical regions other than the motor cortex. For example, studies could be conducted to determine reliable landmarks in the prefrontal cortex and the resulting grid could be used to compare the respective antidepressant efficacy of TMS according to the stimulation of various prefrontal areas. Thus, many opportunities are open to this type of approach to improve TMS practice.

TABLE II. Anatomical limits of the dorsal PMC according to literature data

Rostral limit	PCS (1)	Moore et al., 2000; Schubotz and von Cramon, 2003
	10 mm anterior to the PCS (2)	Fink et al., 1997
Caudal limit	Anterior margin of the CS (3)	Fink et al., 1997; White et al., 1997
	The junction between the anterior third and the two-third posterior of the precentral gyrus (4)	Alkadhi et al., 2002
Dorsal limit	Boundary between the lateral and mesial surfaces of the frontal cortex (5)	Grafton et al., 1996
	Dorsolateral surface of the frontal cortex (6)	Mayka et al., 2006; Tanji and Hoshi, 2009
Ventral limit	Posterior prolongation of the iFS (7)	Grèzes and Decety, 2001; Picard and Strick, 2001
	At a dorsoventral level located between the sFS and the iFS (8)	Rizzolatti et al., 2002; Schubotz and von Cramon, 2003

The numbers between parentheses refer to Figure 10.

REFERENCES

Ahdab R, Ayache SS, Brugières P, Goujon C, Lefaucheur JP (2010): Comparison of "standard" and "navigated" procedures of TMS coil positioning over motor, premotor and prefrontal targets in depressive patients. Neurophysiol Clin 40:27–36.

Alkadhi H, Crelier GR, Boendermaker SH, Golay X, Hepp-Reymond MC, Kollias SS (2002): Reproducibility of primary motor cortex somatotopy under controlled conditions. AJNR Am J Neuroradiol 23:1524–1532.

Amiez C, Kostopoulos P, Champod AS, Petrides M (2006): Local morphology predicts functional organization of the dorsal premotor region in the human brain. J Neurosci 26:2724–2731.

Amunts K, Schleicher A, Bürgel U, Mohlberg H, Uylings HBM, Zilles K (1999): Broca's region revisited: cytoarchitecture and intersubject variability. J Comp Neurol 412:319–341.

Ashburner J, Friston KJ (1999): Nonlinear spatial normalization using basis functions. Hum Brain Mapp 7:254–266.

Binkofski F, Buccino G, Posse S, Seitz R, Rizzolatti G, Freund J (1999): A frontoparietal circuit for object manipulation in man: evidence from an fMRI study. Eur J Neurosci 11:3276–3286.

Chiavaras MM, Petrides M (2000): Orbitofrontal sulci of the human and macaque monkey brain. J Comp Neurol 422:35–54.

de Jong BM, van der Graaf FH, Paans AM (2001): Brain activation related to the representations of external space and body scheme in visuomotor control. Neuroimage 14:1128–1135.

Diekhoff S, Uludağ K, Sparing R, Tittgemeyer M, Cavuşoğlu M, von Cramon DY, Grefkes C (2011): Functional localization in the human brain: Gradient-Echo, Spin-Echo, and arterial spin-labeling fMRI compared with neuronavigated TMS. Hum Brain Mapp 32:341–357.

Ehrsson HH, Geyer S, Naito E (2003): Imagery of voluntary movement of fingers, toes, and tongue activates corresponding body-part-specific motor representations. J Neurophysiol 90: 3304–3316.

Eickhoff SB, Stephan KE, Mohlberg H, Grefkes C, Fink GR, Amunts K, Zilles K (2005): A new SPM toolbox for combining probabilistic cytoarchitectonic maps and functional imaging data. NeuroImage 25:1325–1335.

Eickhoff SB, Amunts K, Mohlberg H, Zilles K (2006): The human parietal operculum. II. Stereotaxic maps and correlation with functional imaging results. Cereb Cortex 16:268–279.

Eickhoff SB, Paus T, Caspers S, Grosbras MH, Evans AC, Zilles K, Amunts K (2007): Assignment of functional activations to probabilistic cytoarchitectonic areas revisited. Neuroimage 36: 511–521.

Fesl G, Moriggl B, Schmid UD, Naidich TP, Herholz K, Yousry TA (2003): Inferior central sulcus: variations of anatomy and function on the example of the motor tongue area. Neuroimage 20:601–610.

Fink GR, Frackowiak RS, Pietrzyk U, Passingham RE (1997): Multiple nonprimary motor areas in the human cortex. J Neurophysiol 77:2164–2174.

Germann J, Robbins S, Halsband U, Petrides M (2005): Precentral sulcal complex of the human brain: Morphology and statistical probability maps. J Comp Neurol 493:334–356.

Geyer S (2004): The microstructural border between the motor and the cognitive domain in the human cerebral cortex. Adv Anat Embryol Cell Biol 174, I-VIII:1–89.

Geyer S, Matelli M, Luppino G, Zilles K (2000): Functional neuroanatomy of the primate isocortical motor system. Anat Embryol (Berl) 202:443–474.

Grafton ST, Fagg AH, Woods RP, Arbib MA (1996): Functional anatomy of pointing and grasping in humans. Cereb Cortex 6: 226–237.

Grèzes J, Decety J (2001): Functional anatomy of execution, mental simulation, observation, and verb generation of actions: A meta-analysis. Hum Brain Mapp 12:1–19.

Grol MJ, de Lange FP, Verstraten FA, Passingham RE, Toni I (2006): Cerebral changes during performance of overlearned arbitrary visuomotor associations. J Neurosci 26:117–125.

Johansen-Berg H, Rushworth MF, Bogdanovic MD, Kischka U, Wimalaratna S, Matthews PM (2002): The role of ipsilateral premotor cortex in hand movement after stroke. Proc Natl Acad Sci USA 99:14518–14523.

Lefaucheur JP (2008): Principles of therapeutic use of transcranial and epidural cortical stimulation. Clin Neurophysiol 119:2179–2184.

Lefaucheur JP (2010): Why image-guided navigation becomes essential in the practice of transcranial magnetic stimulation. Neurophysiol Clin 40:1–5.

Lefaucheur JP (2012): Neurophysiology of cortical stimulation. Int Rev Neurobiol 107:57–85.

Matelli M, Luppino G, Rizzolatti G (1985): Patterns of cytochrome oxidase activity in the frontal agranular cortex of the macaque monkey. Behav Brain Res 18:125–136.

Mayka MA, Corcos DM, Leurgans SE, Vaillancourt DE (2006): Three-dimensional locations and boundaries of motor and premotor cortices as defined by functional brain imaging: a meta-analysis. Neuroimage 31:1453–1474.

Moore CI, Stern CE, Corkin S, Fischl B, Gray AC, Rosen BR, Dale AM (2000): Segregation of somatosensory activation in the human rolandic cortex using fMRI. J Neurophysiol 84:558–569.

Nguyen JP, Lefaucheur JP, Decq P, Uchiyama T, Carpentier A, Fontaine D, Brugiéres P, Pollin B, Féve A, Rostaing S, Cesaro P, Keravel Y (1999): Chronic motor cortex stimulation in the treatment of central and neuropathic pain. Correlations between clinical, electrophysiological and anatomical data. Pain 82:245–251.

Ono M, Kubik S, Abernathey CD (1990): Atlas of the Cerebral Sulci. New York: Georg Thieme Verlag.

Paus T, Jech R, Thompson CJ, Comeau R, Peters T, Evans AC (1997): Transcranial magnetic stimulation during positron emission tomography: A new method for studying connectivity of the human cerebral cortex. J Neurosci 17:3178–3184.

Penfield W, Welch K (1951): The supplementary motor area of the cerebral cortex; a clinical and experimental study. AMA Arch Neurol Psychiatry 66:289–317.

Picard N, Strick PL (2001): Imaging the premotor areas. Curr Opin Neurobiol 11:663–672.

Rademacher J, Burgel U, Geyer S, Schormann T, Schleicher A, Freund HJ, Zilles K (2001): Variability and asymmetry in the human precentral motor system. A cytoarchitectonic and myeloarchitectonic brain mapping study. Brain 124:2232–2258.

Rizzolatti G, Luppino G (2001): The cortical motor system. Neuron 31:889–901.

Rizzolatti G, Luppino G, Matelli M (1998): The organization of the cortical motor system: New concepts. Electroencephalogr Clin Neurophysiol 106:283–296.

Rizzolatti G, Fogassi L, Gallese V (2002): Motor and cognitive functions of the ventral premotor cortex. Curr Opin Neurobiol 12:149–154.

Roland PE, Zilles K (1996): Functions and structures of the motor cortices in humans. Curr Opin Neurobiol 6:773–781.

Rossini PM, Barker AT, Berardelli A, Caramia MD, Caruso G, Cracco RQ, Dimitrijević MR, Hallett M, Katayama Y, Lücking CH, Maertens de Noordhout AL, Marsden CD, Murray NMF, Rothwell JC, Swash M, Tomberg C (1994): Non-invasive electrical and magnetic stimulation of the brain, spinal cord and roots: Basic principles and procedures for routine clinical application. Report of an IFCN committee. Electroencephalogr Clin Neurophysiol 91:79–92.

Sarfeld AS, Diekhoff S, Wang LE, Liuzzi G, Uludağ K, Eickhoff SB, Fink GR, Grefkes C (2012): Convergence of human brain mapping tools: neuronavigated TMS parameters and fMRI activity in the hand motor area. Hum Brain Mapp 33:1107–1123.

Schluter ND, Rushworth MF, Passingham RE, Mills KR (1998): Temporary interference in human lateral premotor cortex suggests dominance for the selection of movements. A study using transcranial magnetic stimulation. Brain 121:785–799.

Schubotz RI, von Cramon DY (2003): Functional-anatomical concepts of human premotor cortex: Evidence from fMRI and PET studies. Neuroimage 20 Suppl 1:S120–131.

Schubotz RI, Anwander A, Knösche TR, von Cramon DY, Tittgemeyer M (2010): Anatomical and functional parcellation of the human lateral premotor cortex. Neuroimage 50:396–408.

Talairach J, Tournoux P (1988): Co-planar Stereotactic Atlas of the Human Brain: 3-Dimensional Proportional System: An approach to Cerebral Imaging. New York: Thieme Medical Publishers.

Tanji J, Hoshi E (2009): Premotor Areas. In: Binder MD, Hirokawa N, Windhorst U, editors. Encyclopedia of Neuroscience. Berlin Heidelberg: Springer-Verlag. p 925–33.

Thyreau B, Schwartz Y, Thirion B, Frouin V, Loth E, Vollstädt-Klein S, Paus T, Artiges E, Conrod PJ, Schumann G, Whelan R, Poline JB; IMAGEN Consortium (2012): Very large fMRI study using the IMAGEN database: sensitivity-specificity and population effect modeling in relation to the underlying anatomy. Neuroimage 61:295–303.

Tomassini V, Jbabdi S, Klein JC, Behrens TE, Pozzilli C, Matthews PM, Rushworth MF, Johansen-Berg H (2007): Diffusion-weighted imaging tractography-based parcellation of the human lateral premotor cortex identifies dorsal and ventral subregions with anatomical and functional specializations. J Neurosci 27:10259–10269.

Toni I, Rushworth MF, Passingham RE (2001): Neural correlates of visuomotor associations. Spatial rules compared with arbitrary rules. Exp Brain Res 141:359–369.

Turner OA (1948): Growth and development of the cerebral cortical pattern in man. Arch Neurol Psychiatry 59:1–12.

Wang Y, Shima K, Sawamura H, Tanji J (2001): Spatial distribution of cingulate cells projecting to the primary, supplementary, and presupplementary motor areas: a retrograde multiple labeling study in the macaque monkey. Neurosci Res 39:39–49.

White LE, Andrews TJ, Hulette C, Richards A, Groelle M, Paydarfar J, Purves D (1997): Structure of the human sensorimotor system. I: Morphology and cytoarchitecture of the central sulcus. Cereb Cortex 7:18–30.

Yousry TA, Schmid UD, Alkadhi H, Schmidt D, Peraud A, Buettner A, Winkler P (1997): Localization of the motor hand area to a knob on the precentral gyrus. A new landmark. Brain 120:141–157.